1. Report No. FHWA/TX-05/0-4827-1	2. Government Accession No.	3. Recipient's Catalog No.
4. Title and Subtitle Feasibility Study of Non-Contact, High-Speed Elastic Property Measurement of Pavements: Theoretical and Experimental Results		5. Report Date December 2005 6. Performing Organization Code
7. Author(s) Aditya Ekbote, Jing Li, Xuemin Chen, and Richard Liu		8. Performing Organization Report No. Report 0-4827-1
9. Performing Organization Name and Address Department of Electrical and Computer Engineering University of Houston 4800 Calhoun Rd. Houston, TX 77204-4005		10. Work Unit No. 11. Contract or Grant No. Project 0-4827
12. Sponsoring Agency Name and Address Texas Department of Transportation Research and Technology Implementation Office P. O. Box 5080 Austin, TX 78763-5080		13. Type of Report and Period Covered Technical Report September 2004 – August 2005 14. Sponsoring Agency Code
15. Supplementary Notes Project performed in cooperation with the Texas Department of Transportation and the Federal Highway Administration. URL: http://tti.tamu.edu/documents/0-4827-1.pdf		

16. Abstract:

Currently, the elastic properties of pavements are measured using FWD and RDDs. These devices use geosensors that need contact with pavement surface when measurements are made. In this project, a laser system has been developed to replace the geosensors in pavement deflection measurement. A Ground Penetrating Radar (GPR) system was also developed for the measurement of elastic properties of asphalt pavement. Several experiments and field tests have been conducted using the developed laser system and the GPR system. Lab tests performed using the Frequency Modulated Continuous Wave (FMCW) GPR and the Pulse GPR indicated a close correlation between the dielectric constant of asphalt and its density. The Pulse GPR was then used to estimate pavement deflection for a 0.3 mile pavement section, and the results were compared with the FWD results. The pavement deflections estimated using the GPR, and those measured using the FWD were found to be within an acceptible range of error.

17. Key Words Pavement elastic properties measurement; GPR method, correlation between elastic property and electrical property	18. Distribution Statement No restrictions. This document is available to the public through the National Technical Information Service, Springfield, Virginia 22161 www.ntis.gov.

19. Security Classif. (of this report) Unclassified	20. Security Classif. (of this page) Unclassified	21. No. of Pages 46	22. Price

Form DOT F 1700.7 (8-72) Reproduction of completed page authorized

This form was electrically by Elite Federal Forms Inc.

Feasibility Study of Non-Contact, High-Speed Elastic Property Measurement of Pavements: Theoretical and Experimental Results

by

Aditya Ekbote, Jing Li, Xuemin Chen, and Richard Liu

Technical Report 0-4827-1

Project Number: 0-4827
Project title: Feasibility Study of Non-Contact, High-Speed Elastic Property Measurement

Performed in cooperation with the
Texas Department of Transportation
and the
Federal Highway Administration

by the

Subsurface Sensing Laboratory
Department of Electrical and Computer Engineering
University of Houston

December 2005

DISCLAIMERS

The contents of this report reflect the views of the authors, who are responsible for the facts and the accuracy of the data presented herein. The contents do not necessarily reflect the official view or policies of the Federal Highway Administration (FHWA) or the Texas Department of Transportation (TxDOT). This report does not constitute a standard, specification, or regulation.

University of Houston
4800 Calhoun Rd.
Houston, TX 77204

ACKNOWLGMENTS

We greatly appreciate the financial support from the Texas Department of Transportation that made this project possible. The support of the project director, Brian Michalk, and program coordinator, Ed Oshinski, are also very much appreciated. We also thank the Project Monitoring Committee members and Dr. German Claros for their encouragement and support to this project.

TABLE OF CONTENTS

LIST OF FIGURES

LIST OF TABLES

Chapter 1: Introduction

1.1 Background and Overview

Currently, the elastic properties of pavements are measured using FWD and RDDs. Both of the FWD and RDD use geosensors for pavement deflection measurements. However, due to the fact that the displacement sensors need physical contact with the materials to be measured, both FWD and RDD vehicles have to be stopped and sensors set up every time measurements have to be made, which makes measurements slow to conduct network level measurements. This also makes it difficult to collect data on an open road. Extreme precaution has to be taken and traffic control has to be enforced prior to the measurements.

In this project, laser sensors are employed to replace geophone sensors for pavement deflection measurement because laser sensors make non-contact measurements and have a very high accuracy in distance measurements. The laser device has been verified to be accurate by comparing with geosensors's results.

To search for better methods that have capability to do measurements at highway speed, a GPR system has been developed to measure the electrical property of pavements. Algorithms for establishing the relationships between the elastic and the electrical properties of pavement materials are also investigated.

The measured results of the laser sensors for pavement deflection measurement will be discussed in Chapter 2. The measured results and correlations with the FWD data will be given in Chapter 3. Conclusions and recommendations are in Chapter 4.

Chapter 2: Measured Results by Laser Device

2.1 Introduction

Traditionally the Falling Weight Deflectometer (FWD) has used geophone sensors for the pavement deflection measurement. In this research, the laser device developed at the University of Houston's Subsurface Sensing Lab was used for measuring the pavement deflections.

2.2 FWD Measurement

The FWD has the capability of storing pavement deflection history for the time interval of 30 ms from the time the load is dropped onto the pavement, as shown in Fig. 2-1. For most applications, only the peak deflections measured by each sensor are used for further analysis. In detail, it can be observed that sensor D1, located at the center of the load plate, records maximum deflection. The deflections recorded by D1, D2, D3, D4, D5, D6 and D7 decrease as the sensors are located away from the point of impact. By processing the measured data, the elastic properties of the pavements can be obtained.

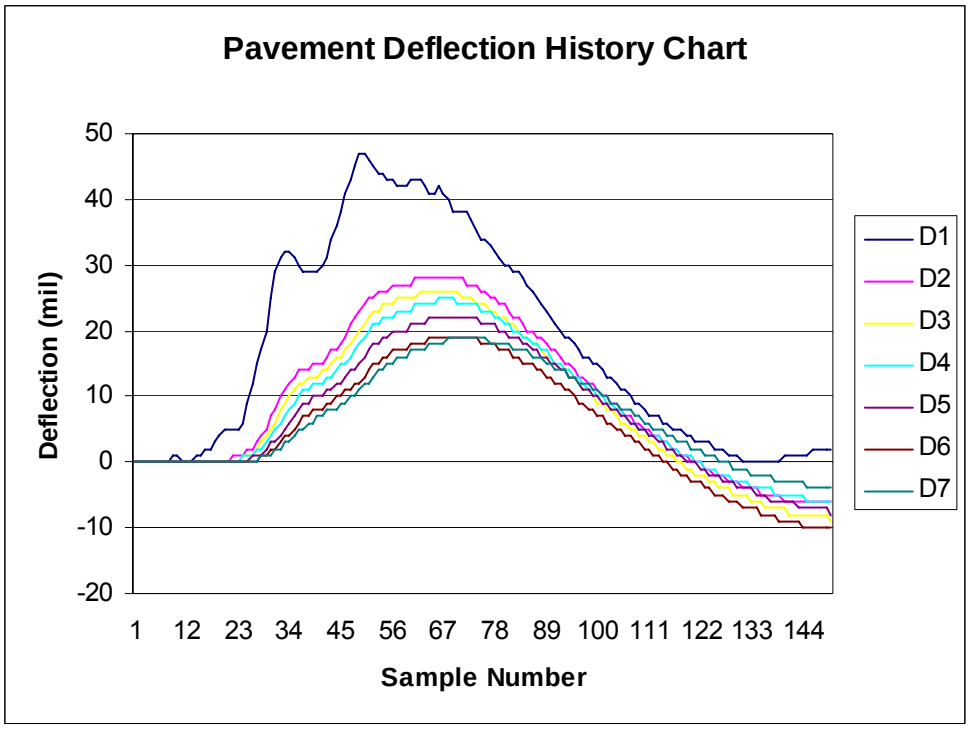

Fig. 2-1 Pavement deflection time history chart

2.3 Laser Device Setup

The laser device was mounted on a push cart and positioned at 20 Inch from the center of the loading plate of the FWD, as shown in Fig. 2-2. Accelerometers were installed on the push cart and the FWD frame to compute and compensate vibrations of the push cart frame when the weight is dropped by the FWD.

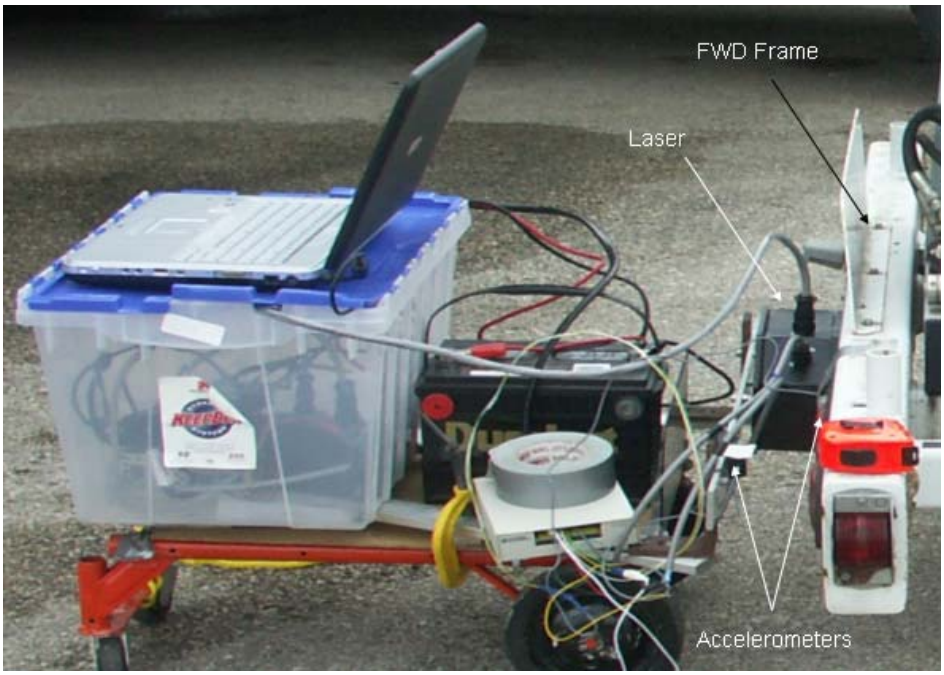

Fig. 2-2 Laser device setup

The FWD was used to apply the load on the pavement five times, with an average force of 16630 lbf. The pavement deflections were measured using the FWD and the laser device at each drop. The vibrations in the laser device frame were measured using the accelerometer mounted on the frame. The acceleration data recorded was integrated twice to get the vibrations in mils. Finally, the pavement deflections measured using the laser were compensated for the laser frame vibration using the measured frame vibration. The pavement deflections using the laser device and the FWD were compared.

2.4 Results Measured by Laser Device and Accelerometers

Fig. 2-3 shows the results obtained for pavement deflections obtained using the laser device for the four FWD drops. The Y-axis represents deflections in mils, and the X-axis represents time in seconds.

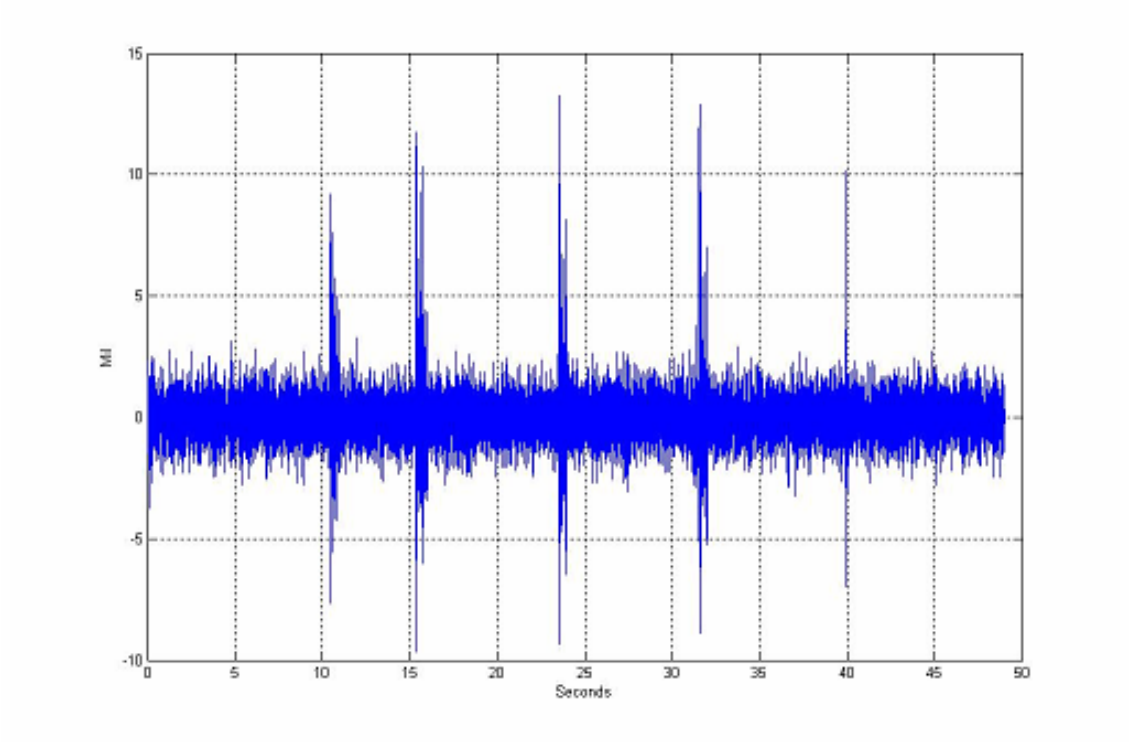

Fig. 2-3 Laser results

Fig. 2-4 shows the laser frame vibrations measured using the accelerometer. The Y-axis represents the vibrations in mils, and the X-axis represents the time in seconds.

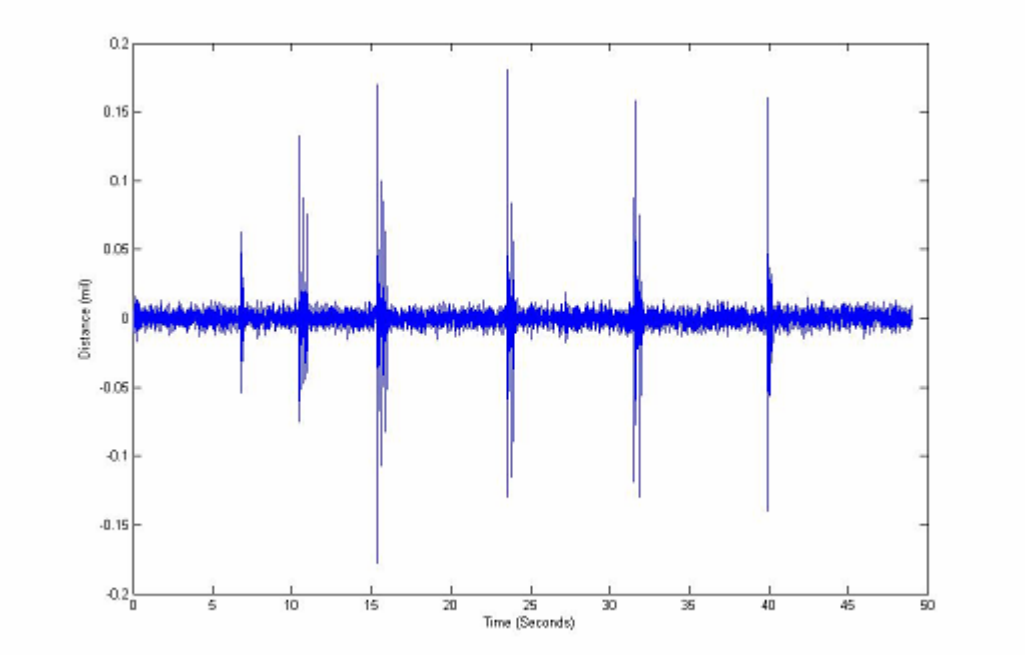

Fig. 2-4 Frame vibrations measured by accelerometer

Fig. 2-4 shows that six vibrations are recorded. The first vibration in the laser frame is recorded when the loading plate is initially lowered as a part of the FWD setup sequence. The average frame vibration recorded by the accelerometer was 0.15 mils.

After compensating the effect of the laser frame vibration from the recorded deflections, the pavement deflections using the laser device and FWD were compared. Table 2-1 shows the results obtained using the FWD and the laser device for deflections measured at 20 inches from the point of load impact.

Table 2-1 Pavement deflections measured by the laser device and the FWD

	Deflections using Laser (mils)	Deflections using FWD (mils)
Drop 1	9.65	12.5
Drop 2	12.17	12.43
Drop 3	13.37	13.05
Drop 4	13.5	13.2
Drop 5	10.15	12.5

The final results verified that the laser device measured results are very close to the results measured by FWD geophone sensors. Laser sensors are verified to be capable of replacing current geophone sensors.

Chapter 3: Measurements by GPR systems

3.1 Introduction

Lab experiments were performed to study the relationship between the density of asphalt and its dielectric constant. These experiments were followed by field tests on test pads using the GPR and the FWD device. The FWD and the GPR data was then processed and compared.

3.2 Verification of the Relation between Density and Dielectric Constant

To confirm the relationship between the density of asphalt slab and its dielectric constant, one of the asphalt slabs was constructed using 960 pounds of asphalt, which was poured into a wooden box 30.75 Inch wide and 64 Inch long, as shown in Fig. 3-1 and Fig. 3-2.

Fig. 3-1 Asphalt slabs for lab experiment

Data was collected several times at different densities using both Frequency Modulated Continuous Wave Radar and Pulse GPR.

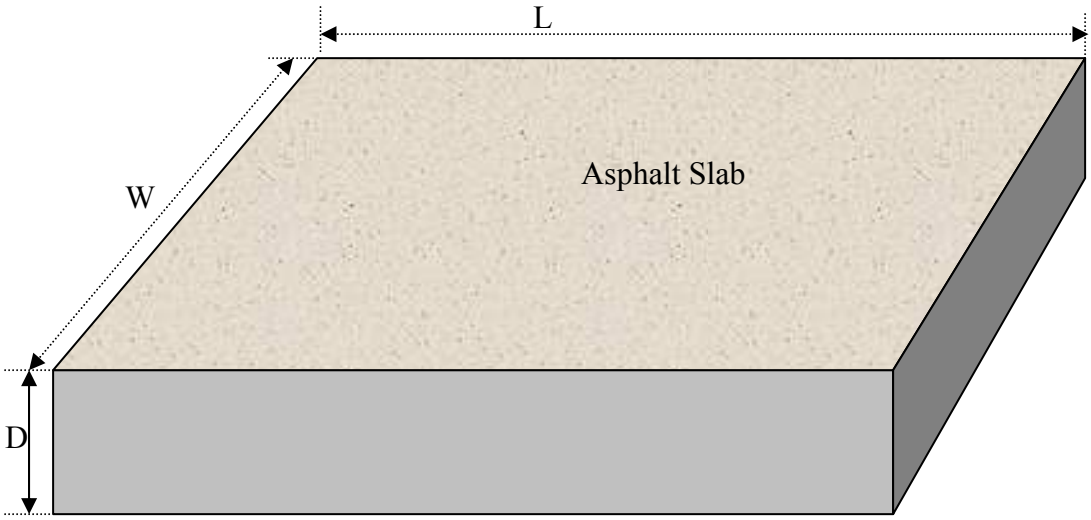

Fig. 3-2 Asphalt slab in the lab, where L = 64 Inch and W = 30.75 Inch

Once the slab was constructed, the initial density was 0.0424 pound/inch^3, and the height of the slab was 11.5 Inch. This was followed by measurement of the dielectric constant of the slab using both the Frequency Modulating Continuous Wave (FM-CW) GPR and Pulse GPR. This collection of steps was called Test 1. A similar procedure was repeated for two more densities by uniformly pressing the asphalt. For Test 2, the height of the slab was pressed to 11 Inch; hence, the density of slab was 0.0443 pound/inch^3. Finally, for Test 3, the height of the slab was 10.75 Inch, and density was 0.0453 pound/inch^3.

3.2.1 Test 1 Results

Test 1 was carried out with 0.0424 pound/inch^3 density of the slab. Fig. 3-3 and Fig. 3-4 show the results obtained with the FM-CW GPR and Pulse GPR, respectively.

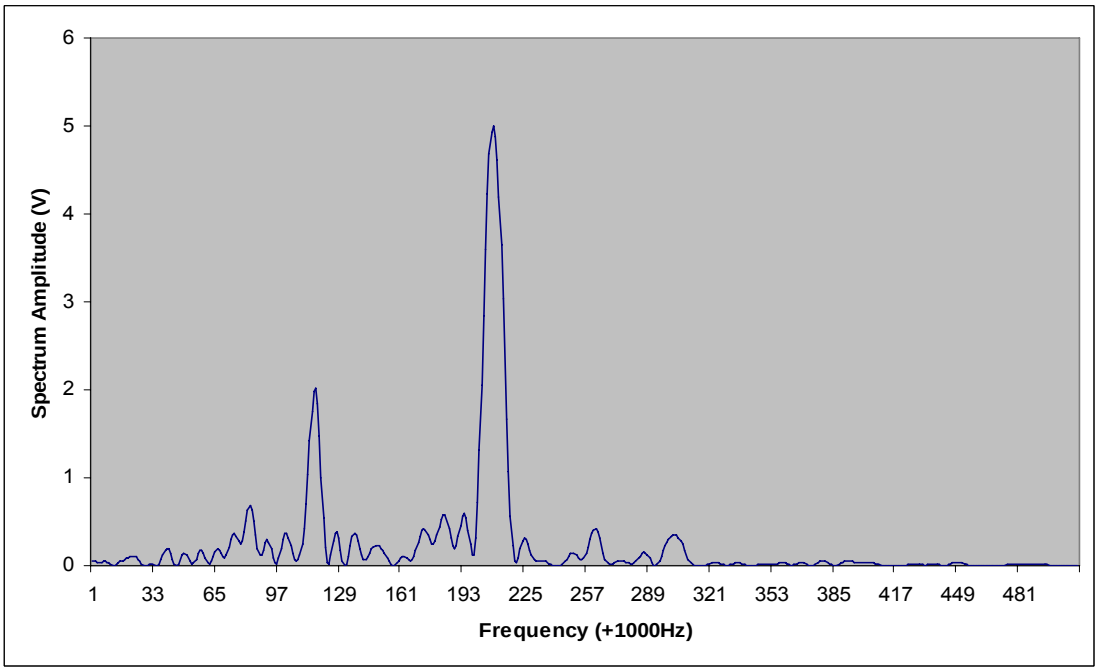

Fig. 3-3 Test 1 using the FMCW radar, slab thickness 11.5 Inch

The dielectric constant of the pavement can be estimated from above FMCW radar data as [3]:

$$\varepsilon_r^{FM\text{-}CW} = (0.04764*(f2-f1)/2*30/2.54/11.5)^2 = 5.065689 \quad (4\text{-}1)$$

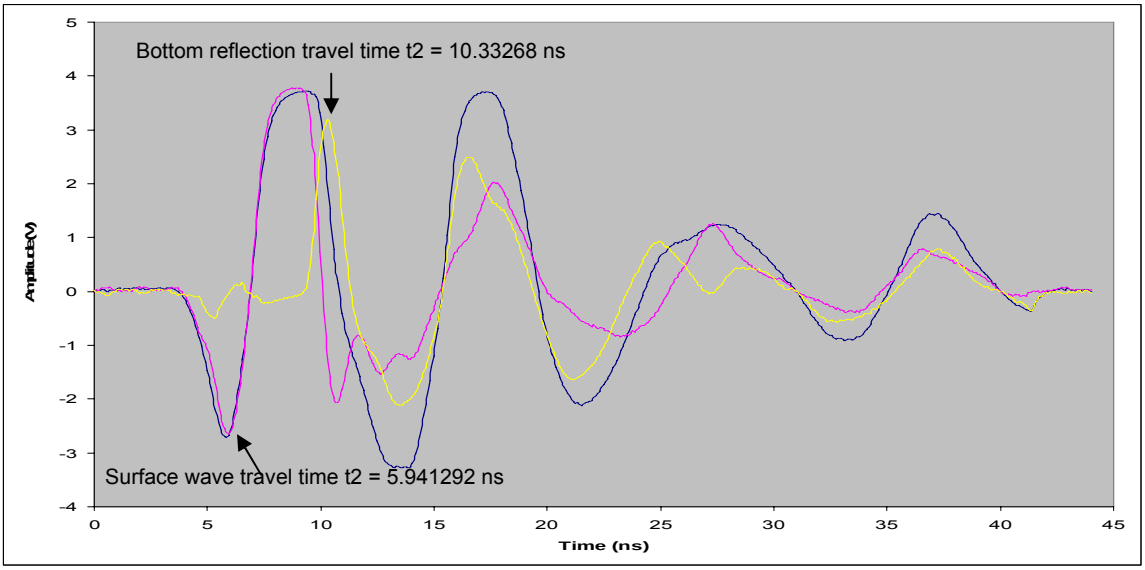

Fig. 3-4 Test 1 using the pulse GPR, slab thickness 11.5 Inch

From pulse GPR data, as shown in Fig. 3-4, the dielectric constant can be calculated by:

$$\varepsilon_r^{PulseGPR} = ((t2-t1)/2*30/2.54/11.5)^2 = 5.085375 \quad (3\text{-}2)$$

3.2.2 Test 2 Results

Test 2 was carried out with 0.0443 pound/inch^3 density of the slab. Fig. 3-5 and Fig. 3-6 show the results obtained with the FM-CW GPR and Pulse GPR, respectively.

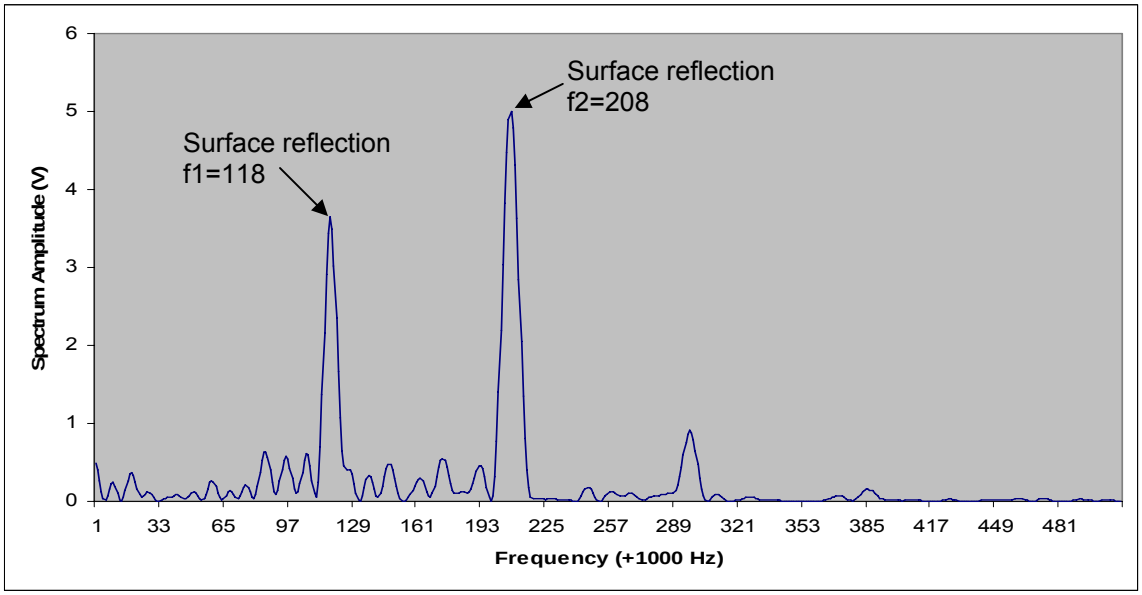

Fig. 3-5 Test 2 of the FMCW radar, slab thickness being pressed to 11 Inch

The dielectric constant can be calculated by:

$$\varepsilon_r^{FM\text{-}CW} = (0.04764*(f2-f1)/2*30/2.54/11)^2 = 5.298565 \quad (3\text{-}3)$$

The dielectric constant is

$$\varepsilon_r^{Pulse} = ((t2-t1)/2*30/2.54/11.5)^2 = 5.342377 \quad (3\text{-}4)$$

3.2.3 Test 3 Results

Test 3 was carried out with 0.0453 pound/inch^3 density of the slab. Fig. 3-7 and Fig. 3-8 show the results obtained with the FM-CW GPR and Pulse GPR, respectively.

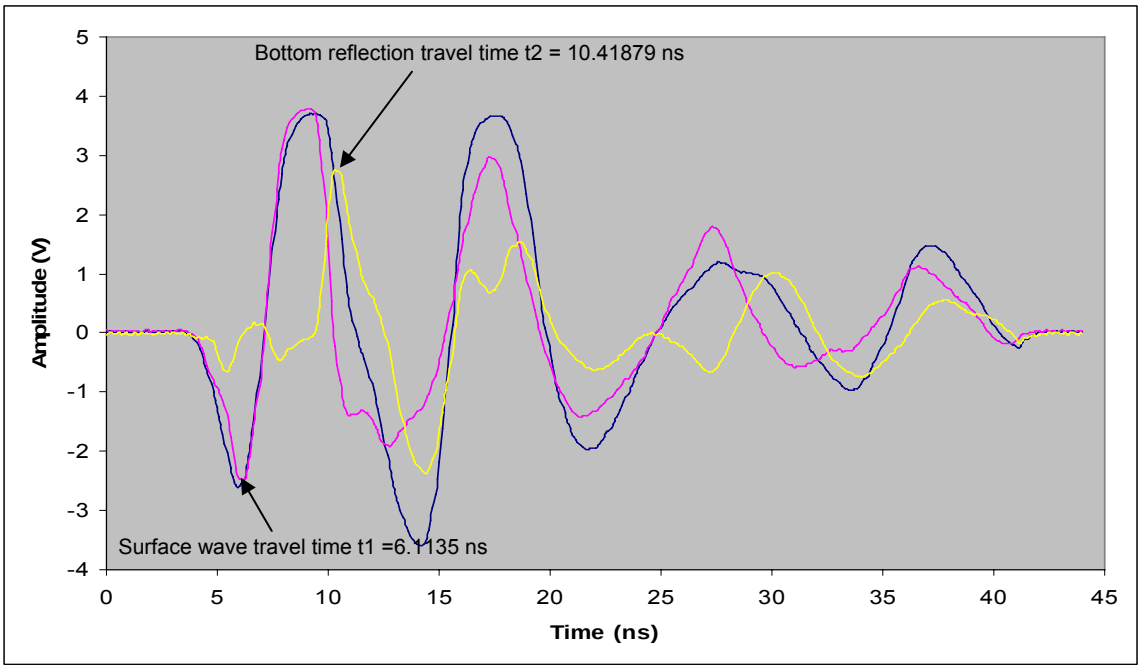

Fig. 3-6 Test 2 of the pulse GPR, slab thickness being pressed to 11 Inch

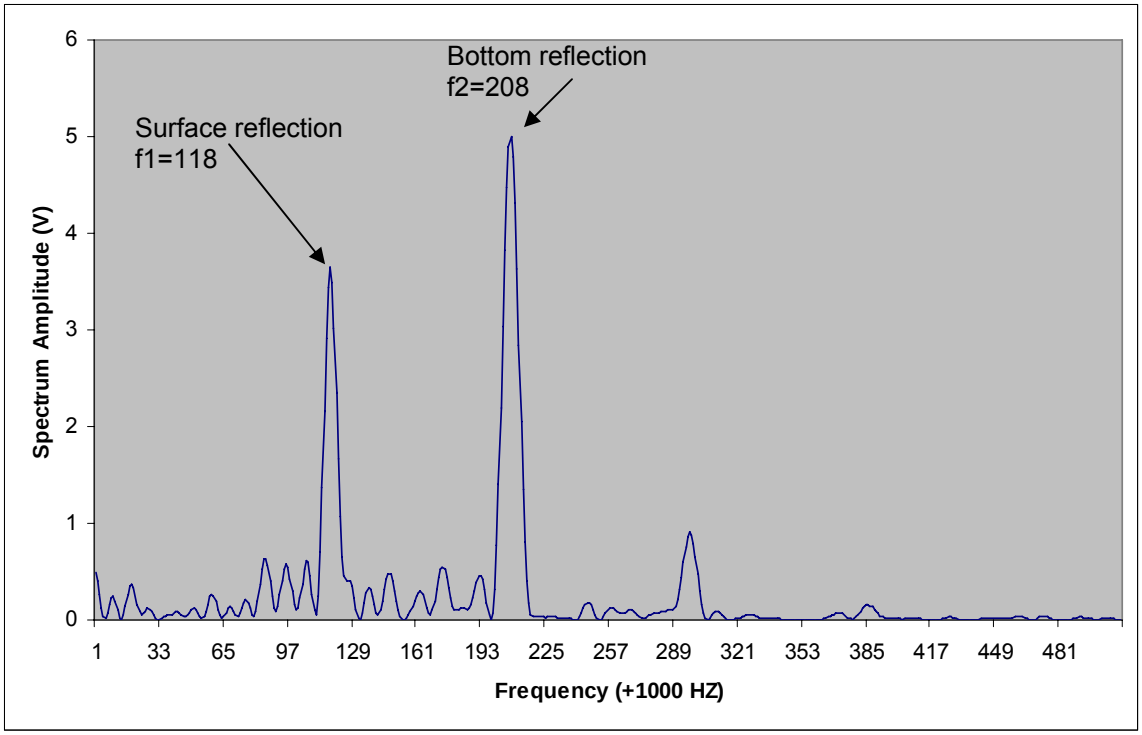

Fig. 3-7 Test 3 of the FMCW radar, slab thickness being pressed to 10.75 Inch

The dielectric constant is

$$\varepsilon_r^{FM\text{-}CW} = (0.04764*(f2-f1)/2*30/2.54/10.75)^2$$
$$= 5.547875 \qquad (3\text{-}5)$$

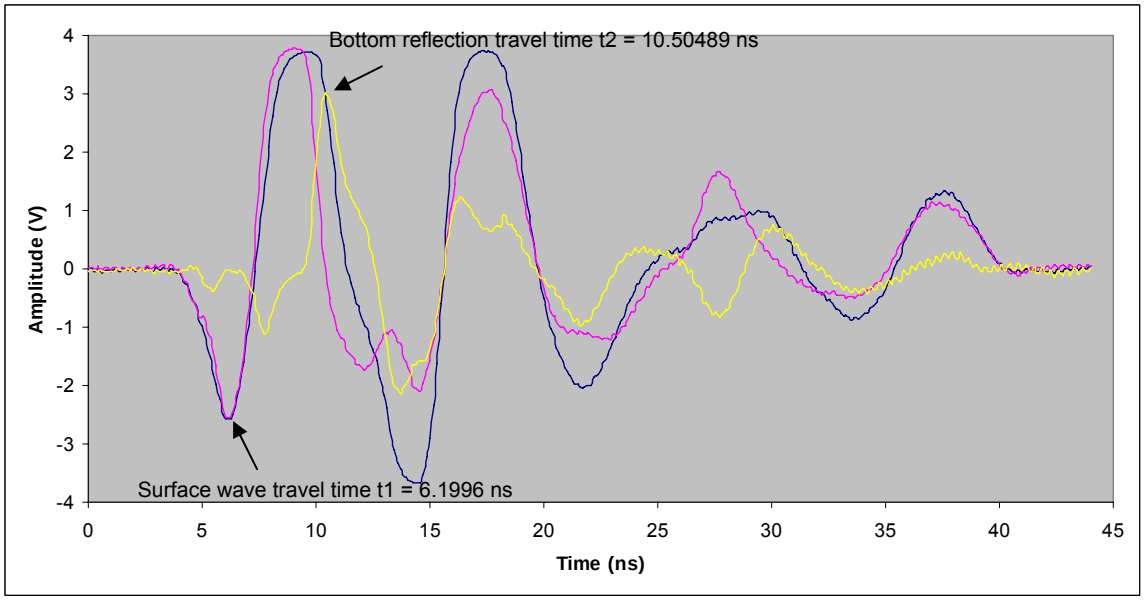

Fig. 3-8 Test 3 of the pulse GPR, slab thickness being pressed to 10.75 Inch

The dielectric constant is

$$\varepsilon_r^{Pulse} = ((t2-t1)/2*30/2.54/10.75)^2$$
$$= 5.593749 \quad (3\text{-}6)$$

3.2.4 Lab Test Data Analysis

After completing all the tests, Equation 4-1 through Equation 4-6 give the dielectric constant of the slab measured by FM-CW radar and pulse GPR at different densities. The dielectric constant calculated was plotted against density, as shown in Fig. 3-9.

Fig. 3-9 evidently shows that the dielectric constant of asphalt is correlated with its density. The correlation is more of a monotonic correspondence. In order to further investigate the correlation between the pavement deflections and GPR data, field tests were performed, as discussed in the following chapters.

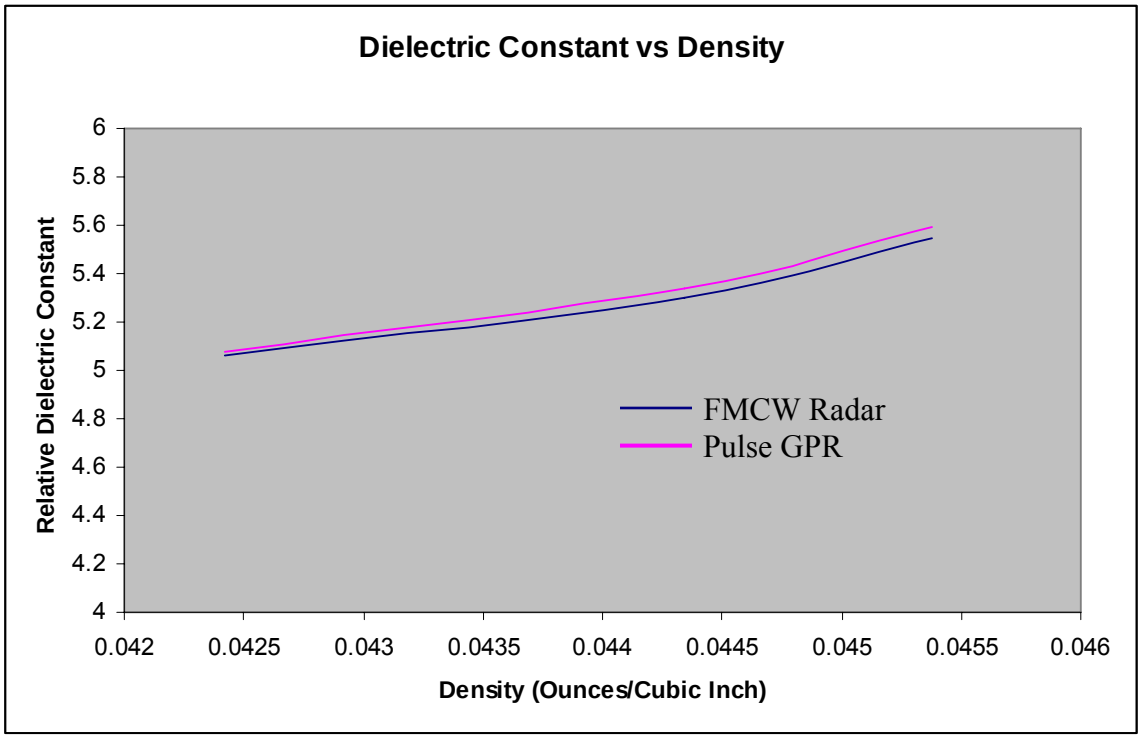

Fig. 3-9 The relation between dielectric constant and density of asphalt material

3.3 Field Tests

All the field tests were performed using the Pulse GPR because of the obvious advantage of the pulse GPR for deeper ground penetration. Henceforth, the Pulse GPR shall only be referred to as GPR.

A series of field tests were performed using GPR and the FWD on several pavement sections. The results obtained using both methods were processed and compared to find an empirical correlation between GPR data and pavement deflections using the FWD.

Four known pavement sections with different Elastic modulus were selected for performing the tests. On each section, first, several GPR traces were collected and stored. The GPR data collection was immediately followed by FWD data collection. This procedure was followed to ensure similar temperature and moisture content conditions.

3.3.1 Tests at Pad 1

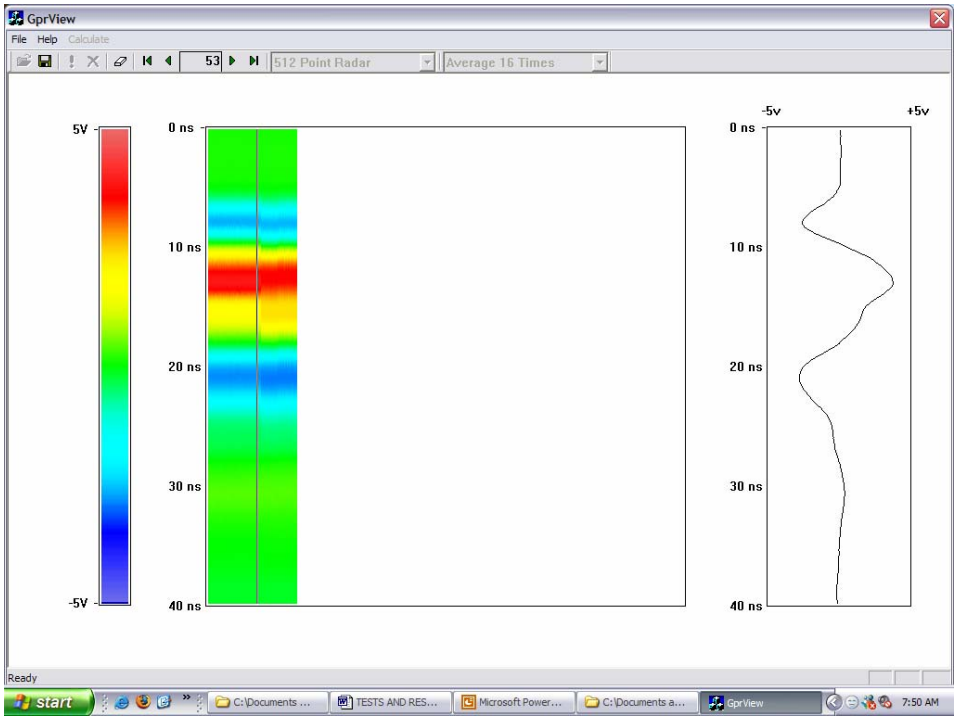

Fig. 3-10 GPR trace color-map obtained at pad 1

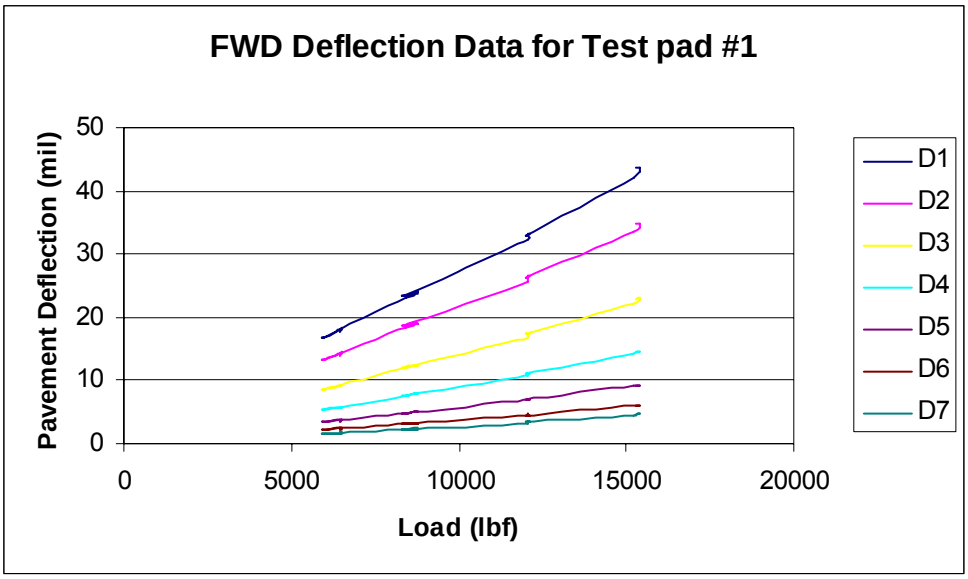

Fig. 3-11 Pavement deflection data obtained with the FWD at pad 1

3.3.2 Tests at Pad 2

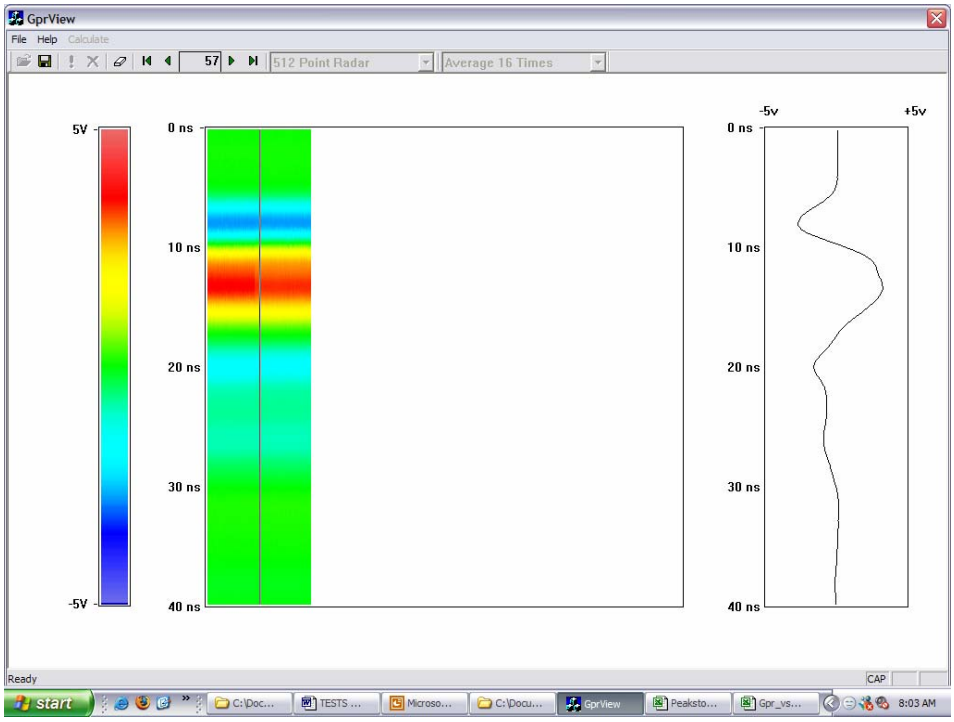

Fig. 3-12 GPR trace color-map obtained at pad 2

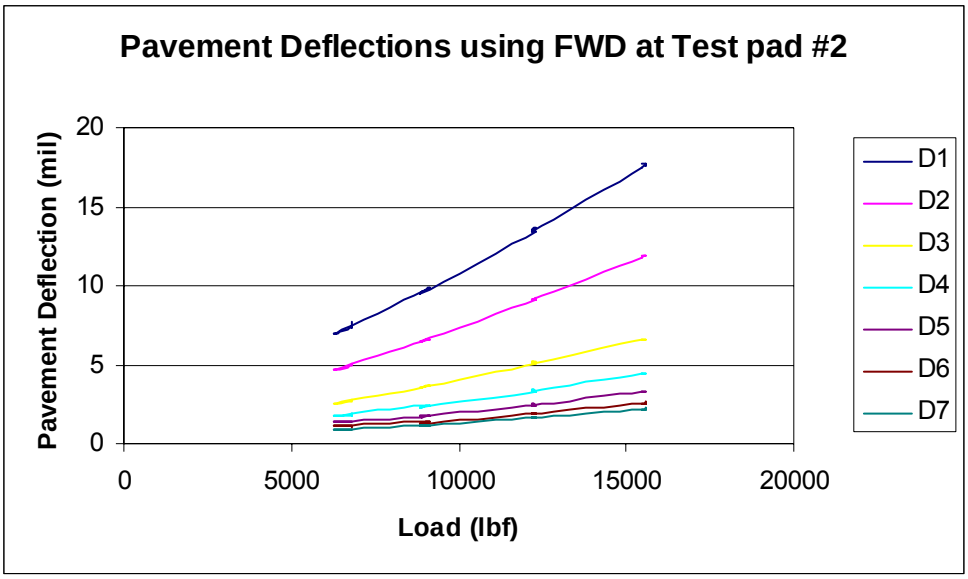

Fig. 3-13 Pavement deflection data obtained with the FWD at pad 2

3.3.3 Tests at Pad 3

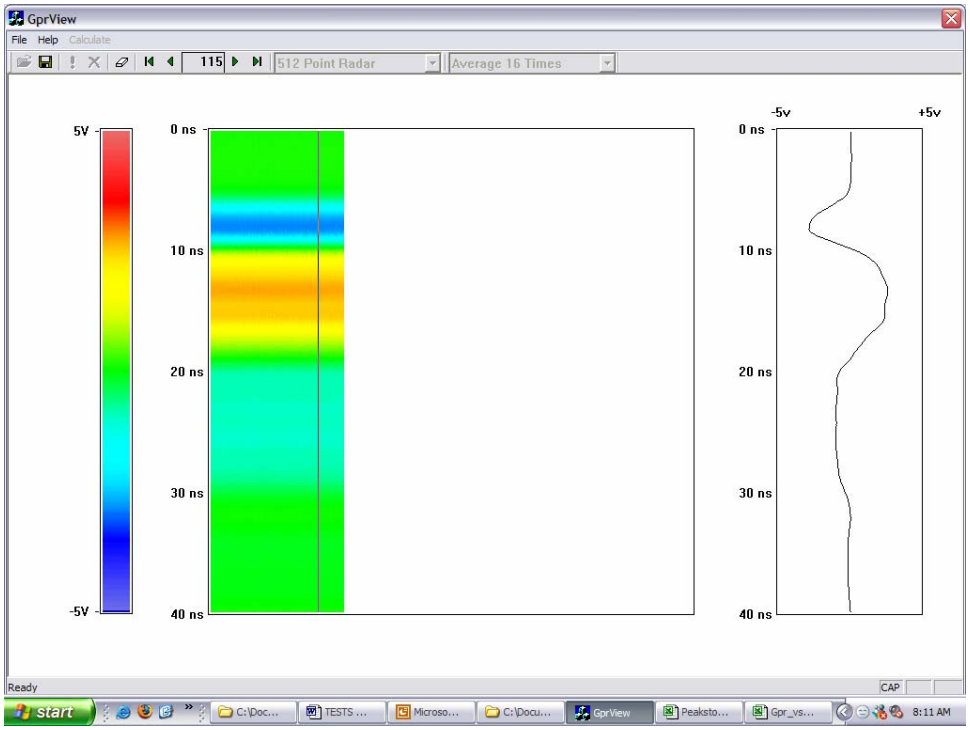

Fig. 3-14 GPR trace color-map obtained at pad 3

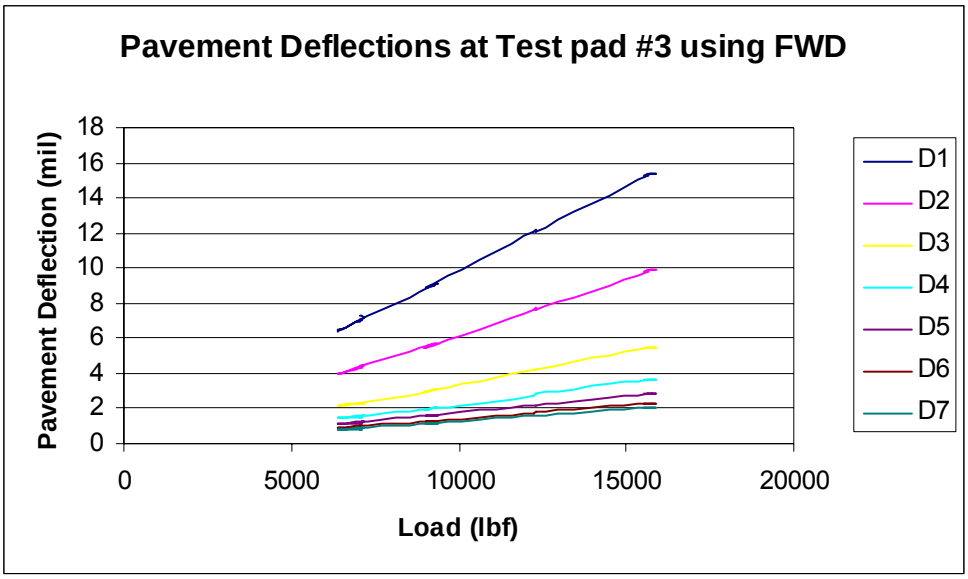

Fig. 3-15 Pavement deflection data obtained with the FWD at pad 3

3.3.4 Tests at Pad 4

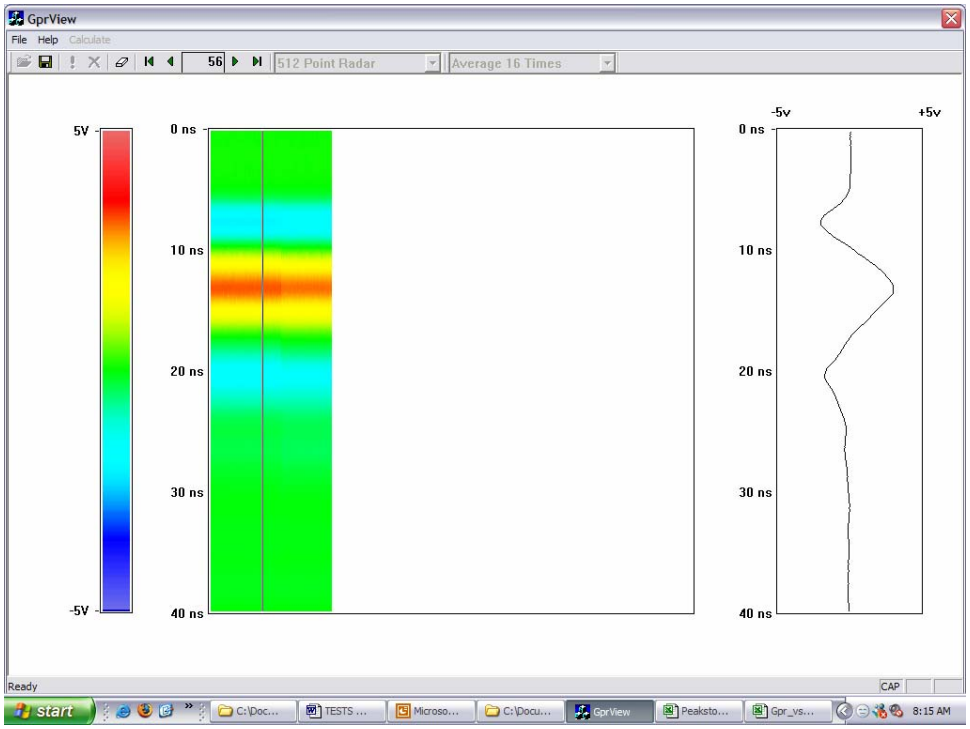

Fig. 3-16 GPR trace color-map obtained at pad 4

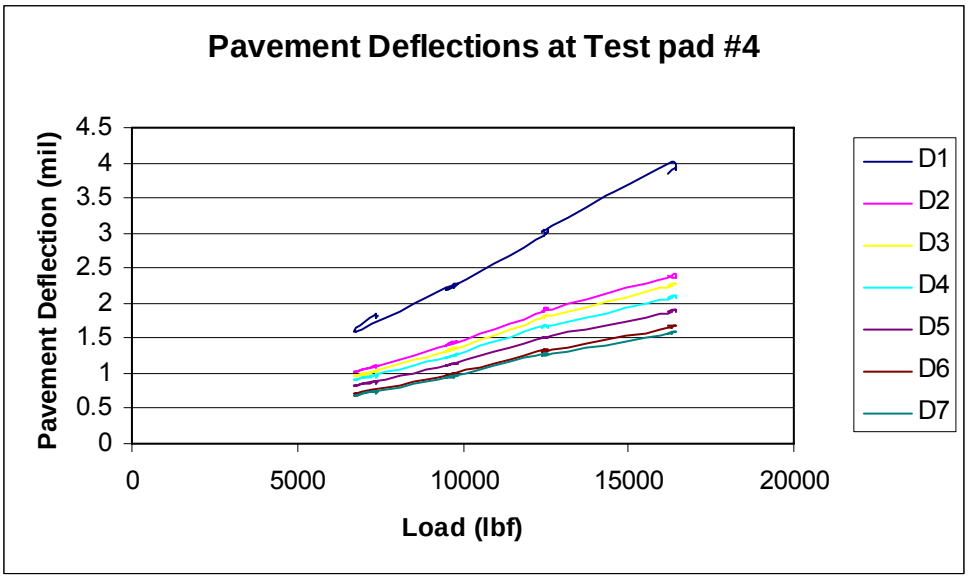

Fig. 3-17 Pavement deflection data obtained with the FWD at pad 4

3.3.5 Data Processing

As discussed in the previous chapter, the travel time of the layer reflections is found to be a function of the dielectric constant of pavement materials. However, in our experiments, we found that the DC offset of the GPR traces is not only related to the dielectric constant of the pavement material but also related to the conductivity. Hence, it is more reliable to DC offset, as an indicator of GPR measurements. Initially, the GPR traces obtained at each test pad were averaged in order to minimize influence of any anomalous GPR traces on the final results. Fig. 3-18 shows the average traces for all the four pads.

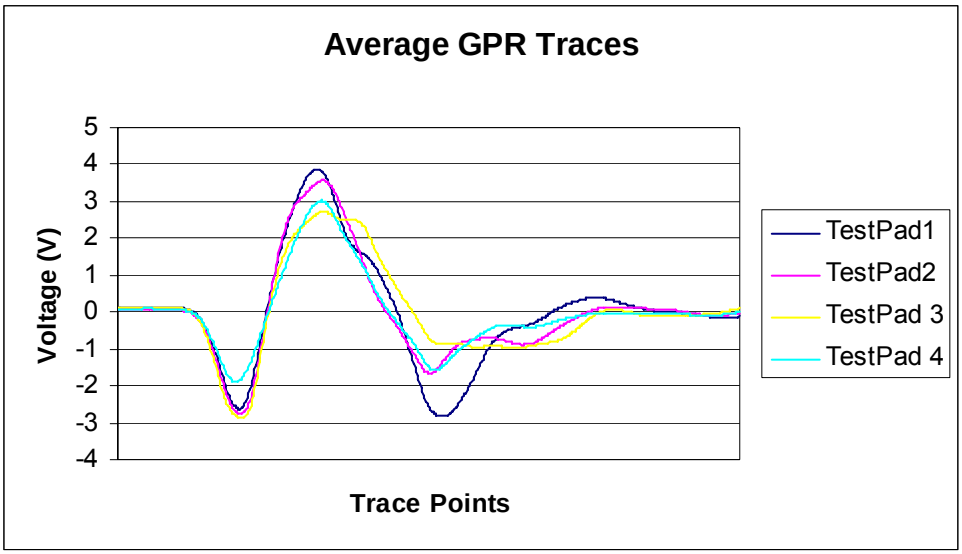

Fig. 3-18 Average GPR traces for all test pads

Then, in order to compute the DC offset voltage of the GPR trace, the voltage data at each point of the trace was summed and divided by number of points in each trace. Table 3-1 shows the GPR DC offset values in voltage along with the FWD data collected for all the seven geophone sensors in mils.

Table 3-1 GPR and FWD collected from four separate test pads

	Pad 1	Pad 2	Pad 3	Pad 4
GPR Trace DC Offset (V)	0.231095	0.087995	0.043123	-0.0589
D7 (mils)	4.56	2.19	2.03	1.58
D6 (mils)	5.98	2.56	2.3	1.67
D5 (mils)	9.16	3.23	2.85	1.89
D4 (mils)	14.6	4.4	3.68	2.08
D3 (mils)	22.91	6.61	5.45	2.25
D2 (mils)	34.72	11.87	9.85	2.39
D1 (mils)	43.55	17.66	15.29	3.85

In order to find correlation between the GPR data and the FWD data, all the data was normalized and plotted together. Table 3-2 shows the normalized data for the GPR and the FWD sensors.

Table 3-2 Normalized GPR and FWD sensor data

	Pad 1	Pad 2	Pad 3	Pad 4
GPR Trace DC Offset	1	0.380774	0.186603	-0.25489
D7	1	0.480263	0.445175	0.346491
D6	1	0.428094	0.384615	0.279264
D5	1	0.35262	0.311135	0.206332
D4	1	0.30137	0.252055	0.142466
D3	1	0.28852	0.237887	0.09821
D2	1	0.341878	0.283698	0.068836
D1	1	0.405511	0.351091	0.088404

After finding the DC offset of each averaged GPR trace, the results were normalized. They were then plotted with normalized deflection results recorded for all four test pads, as shown in Fig. 3-19.

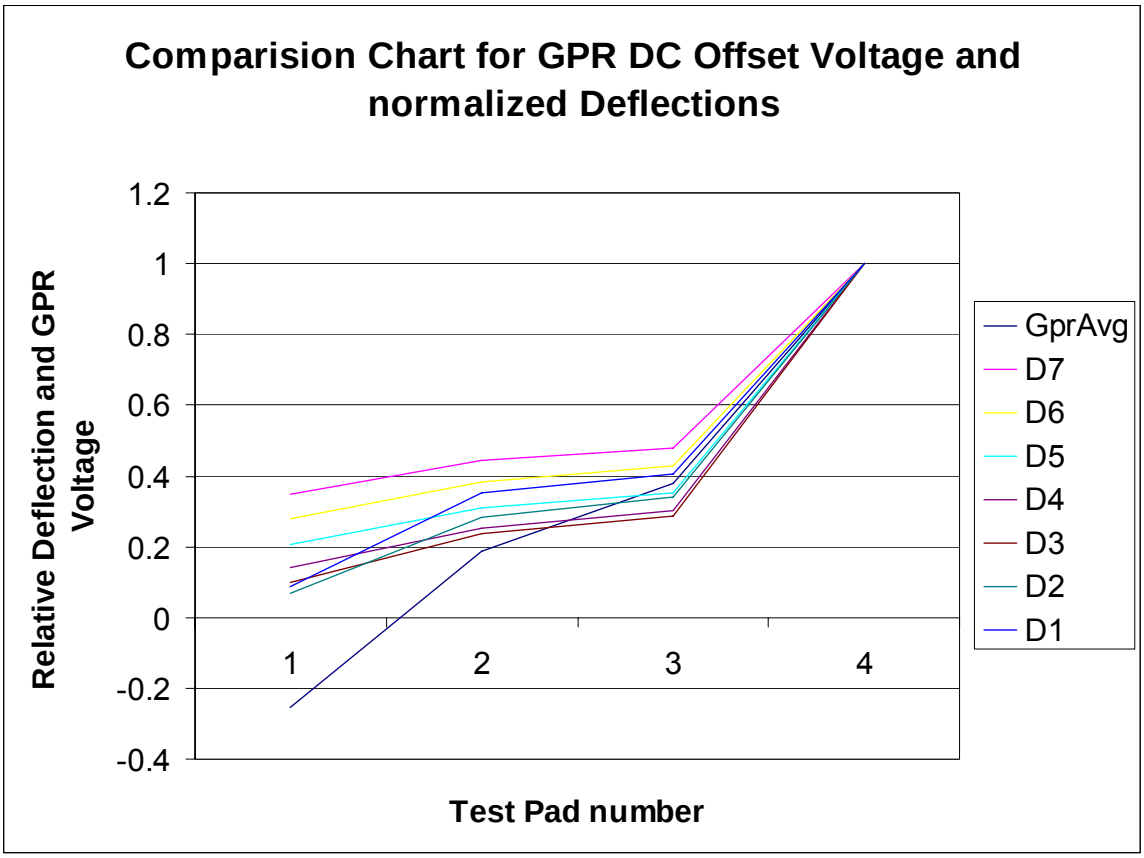

Fig. 3-19 Correlation between GPR data and FWD data

3.3.6 Summary of Field Test Results

The field tests concluded that the pavement deflections have a monotonic correspondence with the GPR data. Also, deflections recorded by geophone D1 appear to be relatively in a closer correlation with the GPR data compared to the other sensors.

3.4 Measurement of Pavement Deflection Using Pulse Ground Penetrating Radar

3.4.1 Introduction

In order to measure the pavement deflections using ground penetrating radar, the empirical relationship found in the previous chapter was utilized to convert GPR results into normalized pavement deflections.

Initially, a section of pavement was selected for the final tests. Fortunately, the pavement was relatively new and, hence, structurally more stable. The section selected was 0.34 miles long. GPR data was collected at every 0.01 miles, discarding a few readings at the beginning and end of the section. This was done primarily to ensure that the FWD data could be collected later at the exact point. In order to ensure accuracy of a distance interval of 0.01 miles between the readings, the DMI was utilized.

After collecting the GPR data, the correlation between the GPR and the FWD found in the previous chapter was used to convert the GPR data into the normalized pavement deflections.

Finally, the FWD was used to measure pavement deflection on the section selected at the same points as where the GPR data was collected. The normalized pavement deflections using both methods were compared and analyzed.

3.4.2 GPR Results

Fig. 3-20 shows one of the GPR data acquired from the pavement section.

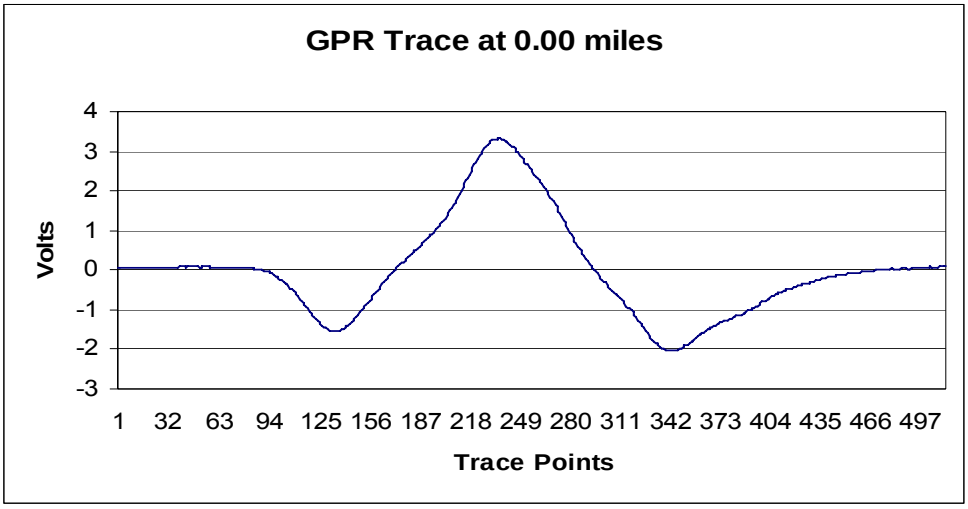

Fig. 3-20 GPR trace acquired at 0.00 miles

As mentioned previously, DC Offset voltage was considered as an indication of GPR measurements. Fig. 3-21 shows a 3D profile of the GPR data acquired, where the x-axis represents number of traces acquired, the y-axis represents GPR voltage in Volts, and the z-axis is the number of Trace points in each trace.

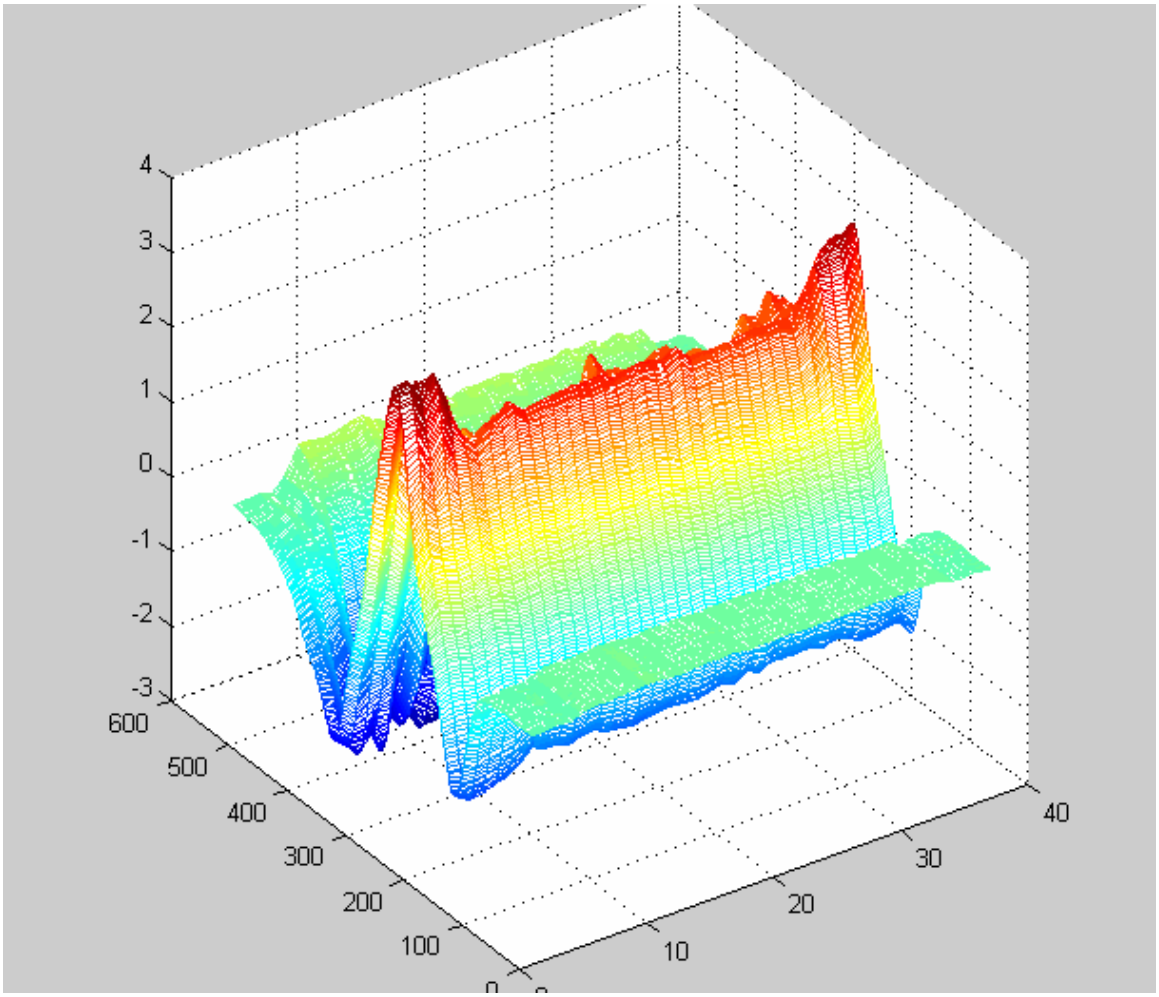

Fig. 3-21 3D profile of the GPR data

After collection of the data, for each trace, all the points were averaged in order to find out the DC Offset of the trace. Fig. 2-22 shows the profile of the DC Offset voltage of all the traces over the pavement section.

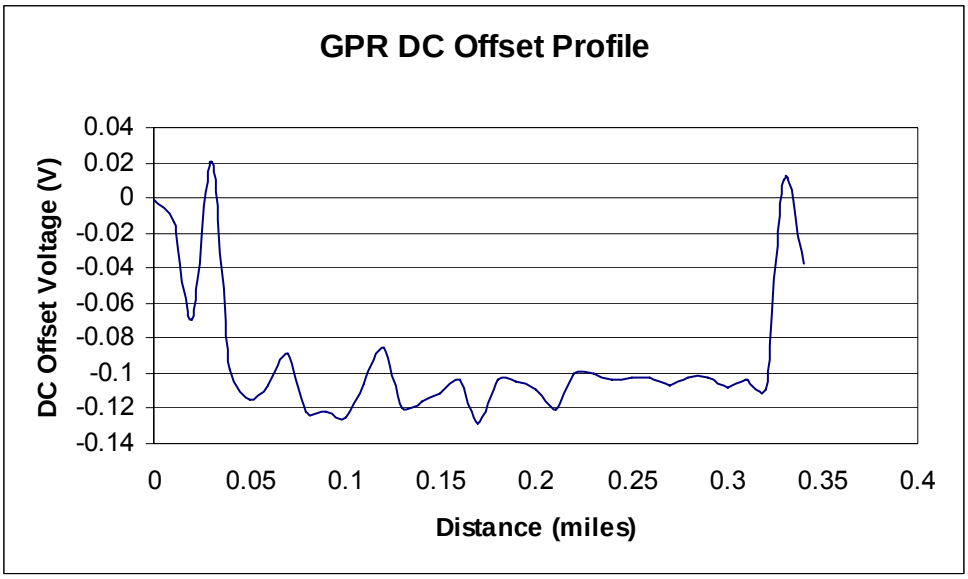

Fig. 3-22 GPR DC offset profile

3.4.3 Data Processing

As discussed before, a few measured points were removed from the beginning and the end of the profile, and the rest of the data was normalized. Fig. 3-23 shows the profile of the normalized data.

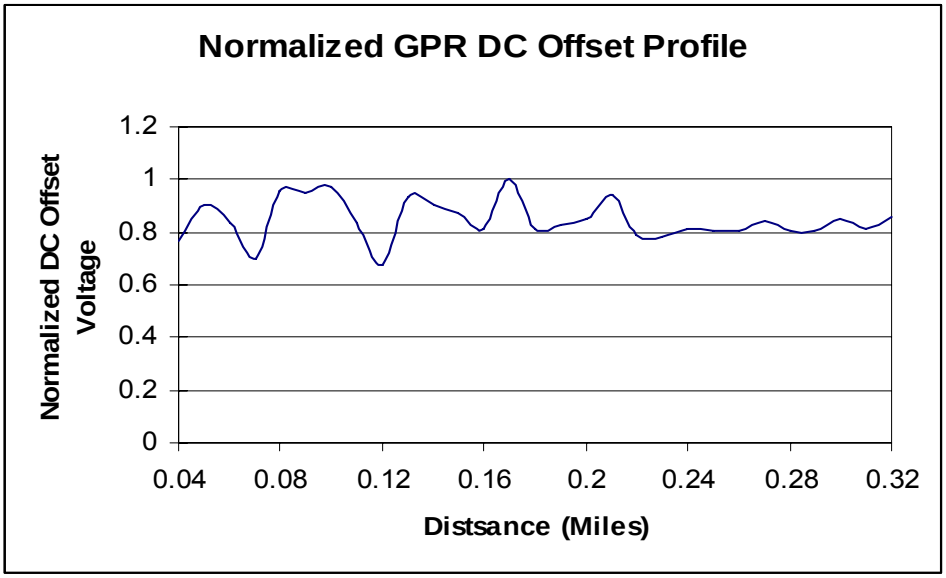

Fig. 3-23 Normalized GPR DC offset profile

The normalized GPR data was mapped linearly using the correlation between the GPR data and the FWD found in section 3.3.5. The mapping was performed to get normalized pavement deflections from the GPR data. The following equations were used for the linear mapping:

$$Y = 0.953*X + 0.046 \quad (3\text{-}7)$$

$$Y = 0.300*X + 0.294 \quad (3\text{-}8)$$

$$Y = 0.595*X + 0.462 \quad (3\text{-}9)$$

where Y is the estimated pavement deflection, and X is the measured GPR data.

Equation 3-7 was used when the normalized GPR data was greater than 0.38, Equation 3-8 was used when the normalized GPR data was greater than 0.186 but less than 0.38, and Equation 3-9 was used when the GPR data was less than 0.186.

The equations mentioned above were used to calculate the normalized pavement deflections using the GPR data collected. Fig. 3-24 shows the profile of the calculated pavement deflections using GPR.

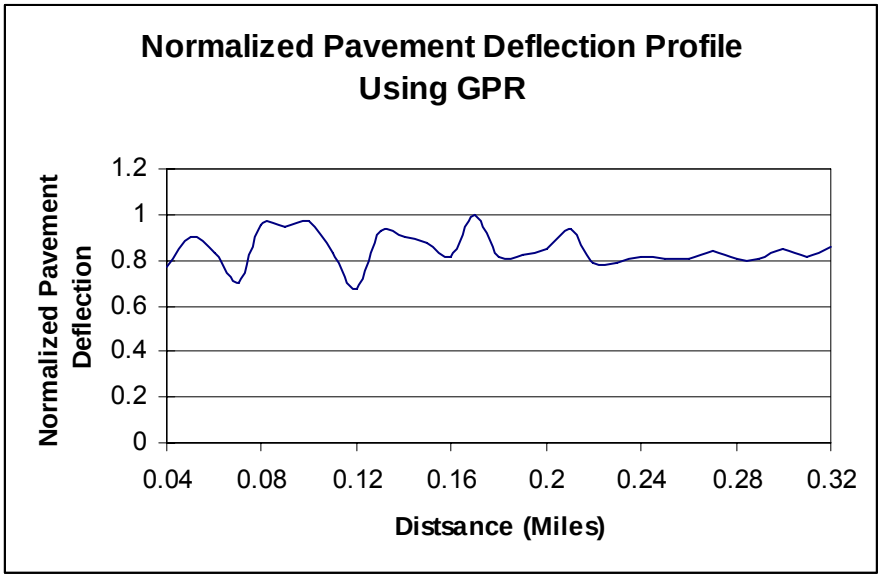

Fig. 3-24 Pavement deflections calculated using GPR

3.5 Measurement of Pavement Deflection Using Falling Weight Deflectometer

The FWD was employed to measure pavement deflections physically over the same pavement section. The DMI and GPS system, also installed on the FWD vehicle, ensured the precise distance and position of measurement points. Table 3-3 shows the measured pavement deflections.

Table 3-3 Pavement deflections using falling weight deflectometer

Distance (miles)	LOAD (lbf)	D1 (mils)	D2 (mils)	D3 (mils)	D4 (mils)	D5 (mils)	D6 (mils)	D7 (mils)
0	18186	22.76	13.84	9.25	7.09	5.44	4.24	3.46
0.01	18317	23.34	13.58	8.75	6.7	5.1	3.95	3.24
0.02	18063	21.98	13.2	8.62	6.55	4.89	3.69	3
0.03	17928	24.5	14	9.2	7.09	5.32	4.1	3.37
0.04	18250	19.5	11.41	7.31	5.77	4.61	3.8	2.99
0.05	18011	19.56	11.07	7.39	5.87	4.43	3.42	2.88
0.06	17976	19.51	11.43	7.4	5.79	4.52	3.52	2.94
0.07	17749	28.63	17.56	9.93	7	5.15	3.99	3.34
0.08	18007	24.24	11.42	5.7	4.65	3.77	3.09	2.65
0.09	18007	15.9	8.06	5.13	4.33	3.54	2.84	2.39
0.1	17884	18	10.09	6.89	5.56	4.46	3.71	3.29
0.11	17876	16.81	9.82	6.34	4.95	3.87	3.05	2.56
0.12	17769	21.72	12.7	6.89	5.02	3.82	3.03	2.58
0.13	18019	17.28	9.88	6.56	5.09	3.89	3.02	2.46
0.14	17868	21.04	12.27	7.45	5.39	3.98	3.1	2.6
0.15	17729	25.46	14.24	7.95	5.5	3.97	3.04	2.56
0.16	17853	18.95	11.16	6.71	4.98	3.71	2.8	2.28
0.17	17916	17.54	9.68	5.82	4.34	3.25	2.48	2.03
0.18	17666	21.93	12.97	7.67	5.41	3.85	2.89	2.36
0.19	17793	19.59	11.02	6.67	4.76	3.58	2.8	2.31
0.2	17527	24.69	14.26	8.56	5.78	4.28	3.26	2.65
0.21	17817	22.96	13.62	8.54	6.19	4.62	3.59	2.91
0.22	17634	27.03	15.69	9.76	7.15	5.28	3.92	3.11
0.23	17785	22.76	12.45	7.95	5.92	4.3	3.24	2.63
0.24	17646	23.89	13.19	8.59	6.52	4.7	3.6	2.98

Table 3-3 Pavement deflections using falling weight deflectometer *(continued)*

0.25	17551	27.02	14.86	9.18	6.67	4.77	3.53	2.84
0.26	17797	18.84	10.1	6.75	5.53	4.36	3.35	2.68
0.27	17721	21.98	13	8.78	6.93	5.34	4.09	3.2
0.28	17841	20.54	11.24	7.02	5.65	4.12	3.08	2.66
0.29	17412	27.81	16.52	10.17	7.43	5.29	3.84	3.04
0.3	17523	27.18	14.81	8.54	6.24	4.62	3.52	2.78
0.31	17416	26.79	14.94	9.58	7.34	5.41	3.89	2.97
0.32	17535	23.74	12.84	7.17	5.01	3.63	2.76	2.28
0.33	17666	20.38	10.72	6.66	5.04	3.78	2.84	2.31
0.34	17308	35.48	19.7	9.41	5.83	3.81	2.87	2.38
0.35	17138	36.46	21.34	10.34	6.36	4.21	3.09	2.64
0.36	17078	43.93	21.36	10.66	7.26	4.89	3.51	2.85

The pavement deflections measured for geophone D1 were normalized and plotted, as shown in Fig. 3-25.

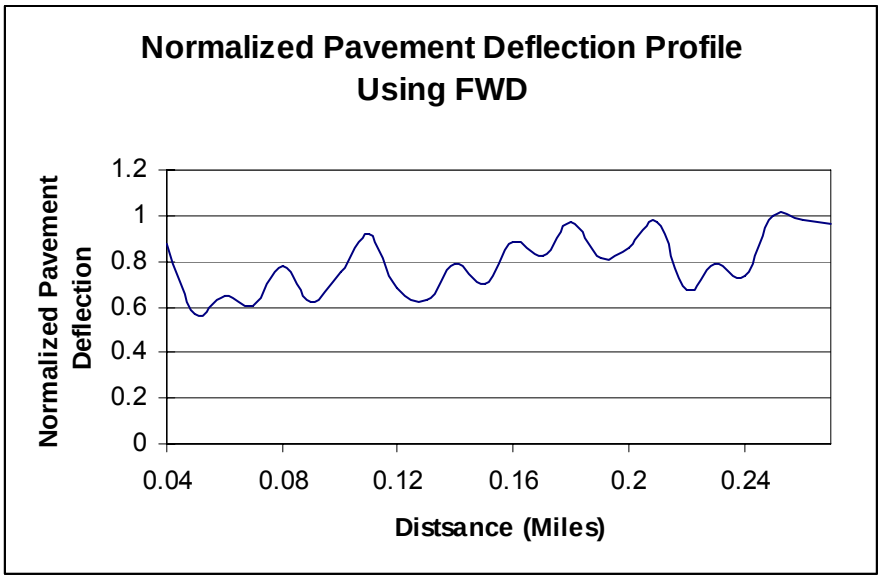

Fig. 3-25 Normalized pavement deflections using FWD

3.6 Comparison Between Pavement Deflections Measured Using FWD and GPR

The results obtained using both methods were compared with each other. Fig. 3-26 shows the profile of the deflections measured using the GPR and the FWD.

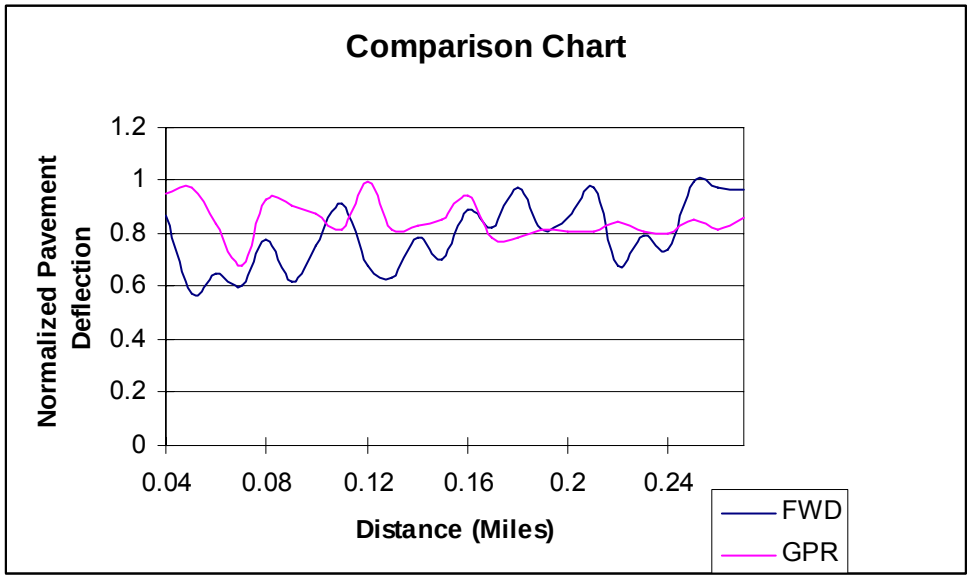

Fig. 3-26 Comparison between results obtained using the GPR and the FWD

The relative error between the measurements using FWD and GPR was under the acceptable range. For 80% of the measurements, the relative error was below 0.2. Fig. 3-27 shows the column chart with the measurements and relative error for each measurement.

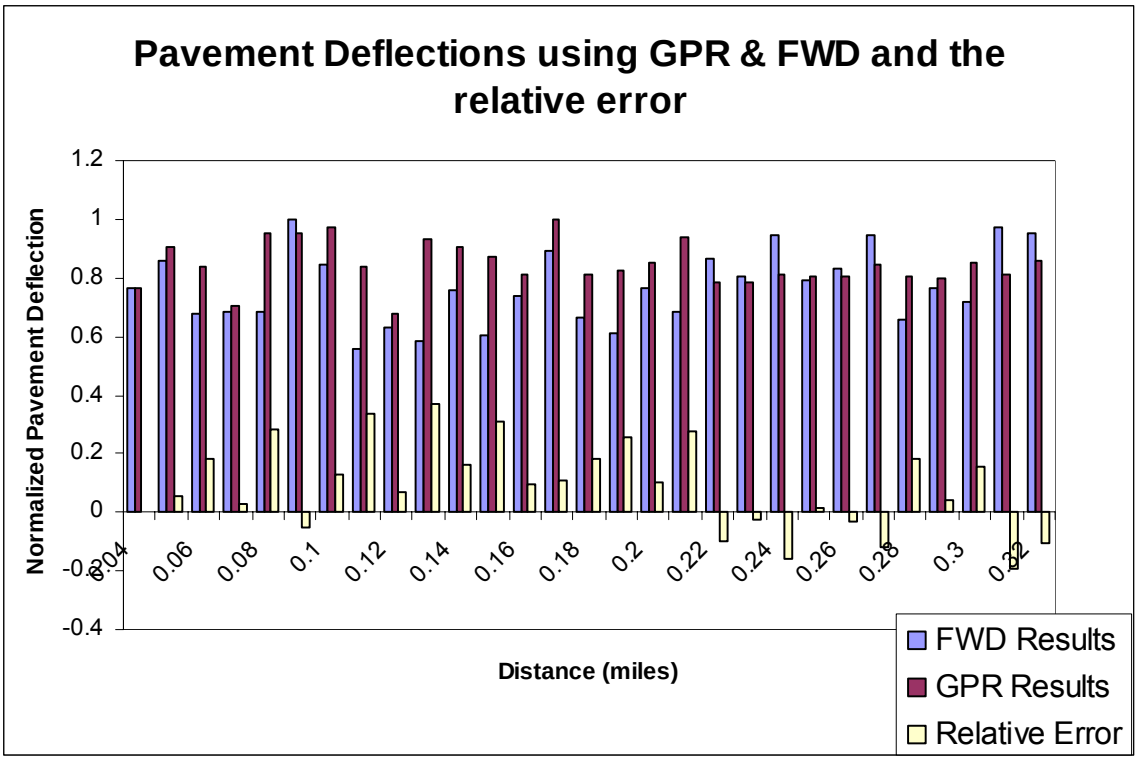

Fig. 3-27 Pavement deflection results with relative error

The results obtained using the GPR agreed with the FWD results to a large extent. This confirmed that there exists a correlation between the electrical properties and the elastic properties of pavement materials. Although, in order to correctly estimate pavement deflections using the GPR, it is required that we use correlation obtained from a similar kind of pavement structure. This shows that presently the GPR can be used as a device for preliminary determination of non-homogenous characteristics in the pavement sections. If the pavement sections are found to be non-homogenous, further tests can be performed using the FWD. This procedure will reduce a lot of time and effort when measuring elastic characteristics on longer pavement sections of a few miles or more.

Chapter 4: Conclusions

The laser sensor method is verified to be able to replace geophone sensors in measuring deflections of pavements. With the compensation of the accelerometer data of the laser frame, the measured deflections by laser sensors agree very well with geophone sensors.

For GPR system, lab experiments revealed a close relation between the dielectric constant of asphalt and its density. Both FMCW and Pulse GPR were used to measure the dielectric constant for different densities, and the results showed a monotonic correspondence between the dielectric constant and density of asphalt.

In the field tests, the FWD was used to measure the pavement deflection that is used as a reference for building the correlation between GPR measurements and FWD results. The estimated and measured pavement deflections were close and within an acceptable error. However, these correlations were not measured in conjunction. In the case of actual pavements, there are several pavement layers involved, including the asphalt surface, base, sub-base and sub-grade. Even though the correlation between the dielectric constant and asphalt density should ideally remain the same, the pavement deflections are not entirely occurring due to the top asphalt layer. If the pavement structure used for mapping the correlation between the FWD and the GPR is different than the structure on which the actual measurements are done, the correlation is relatively weaker.

References

[1] T.Chung, C.Carter, T. Masliwec, and D. Manning. “Impulse Radar Evaluation of Concrete, Asphalt and Waterproofing Membrane.” *IEEE Transactions of Aerospace and Electronic Systems*, Vol. 30, No. 2, pp. 404-415, April 1994.

[2] T. Saarenketo. “Ground penetrating radar Technique in Asphalt Pavement Density Quality Control.” GPR 1998 Proc., Kansas.

[3] C.Liu, J. Li, X. Gan, H. Xing, and X. Chen. “New Model for Estimating the Thickness and Permittivity of Subsurface Layers from GPR Data.” *IEE Proc. – Radar, Sonar and Navigation*, Vol. 149, No. 6, pp. 315-319, December 2002.